Frequency-Temperature-Load Capacitance Behavior of Resonators for TCXO Application

ARTHUR BALLATO, SENIOR MEMBER, IEEE

Abstract—**The effective frequency-temperature curve of a crystal resonator operated with series load capacitance differs from that of the crystal alone. Since the principal method of compensating for the crystal frequency-temperature behavior in a temperature compensated crystal oscillator (TCXO) employs series varactors and a temperature-sensitive compensation network, it is of major importance to be able to understand and deal with this effect in the design of TCXO's. The necessary formulas and discussion are given in this paper.**

Introduction

THE TEMPERATURE compensated crystal oscillator (TCXO) is a modern, cost-effective device capable of realizing frequency stabilities of a few parts in 10^8 over a wide temperature range in a small size [1]-[8]. It incorporates a temperature sensor and associated circuitry to derive a correction signal that is used to compensate the oscillator for the thermal behavior of the crystal vibrator. The method most used for producing the correction consists in adjusting a varactor in series with the vibrator.

For the design of the compensation network it is necessary to know with some accuracy the frequency-temperature ($f - T$) characteristic of the crystal to be compensated. It is found experimentally, however, that the effective $f - T$ curve shape of the crystal-load capacitor series combination alters with the type and value of load capacitor used. This has necessitated empirical rules to accommodate the effect of the $f - T$ curve shape change into workable designs.

In this paper the $f - T$ curve change is explained analytically and shown to arise primarily from two factors: location of operating (load) frequency with respect to crystal resonance and antiresonance frequencies, and temperature coefficient difference between the load and crystal capacitances. Within the single-mode, one-dimensional approximation, we give exact and simple but accurate approximate equations that enable the $f - T$ behavior of the crystal-capacitor composite to be determined in a quantitative manner. Mass-loading effects are included. Sample design charts are provided, with a worked example.

Frequency Equations

Virtually all current TCXO applications employ thickness mode quartz vibrators. For this class of vibrator, excited by an electric field in the thickness direction, the input admittance, assuming no loss and a single driven mode, is

$$Y = j\omega C_0/(1 - k^2 \tan X/X) \tag{1}$$

In (1),

$$C_0 = \epsilon A/2h \tag{2}$$

where C_0 is the vibrator static capacitance, ϵ is the effective permittivity, A is the electrode area, and $2h$ is the thickness. The quantity k is the piezoelectric coupling factor, while X is defined as

$$X = (\pi/2)(f/f_{A0}^{(1)}) \tag{3}$$

with f the frequency variable ($= \omega/2\pi$), and $f_{A0}^{(1)}$ the antiresonance frequency at the fundamental harmonic ($M = 1$), in the absence of mass-loading.

The antiresonance frequencies are sometimes referred to as the mechanical resonances, these being the frequencies for which an open-circuited resonator is an integer number of half-wavelengths in thickness. If the crystal vibrator plate is of density ρ, and the mode under consideration has elastic constant $\bar{c}$ (piezoelectrically stiffened), then the antiresonance frequencies are

$$f_{A0}^{(M)} = M(\bar{c}/\rho)^{1/2}/4h. \tag{4}$$

The harmonics of (4) are integrally related in the absence of mass-loading (negligible electrode coatings); each harmonic corresponds to a pole of the tangent function in (1).

Setting the denominator of (1) equal to zero yields the normalized resonance frequencies as roots of the equation [9]

$$\tan X = X/k^2. \tag{5}$$

The roots of (5), denoted $X_{R0}^{(M)}$, are not harmonically related; the resonance frequencies are then obtained from the $X_{R0}^{(M)}$ by means of (3).

Insertion of a load capacitor C_L in series with the vibrator modifies (1), but the entire effect may be subsumed into changes in the values of C_0 and k^2. Denoting the effective values of C_0 and k^2 in the presence of C_L as C_{0L} and k_L^2, respectively, and defining the quantity α as

$$\alpha = C_0/(C_0 + C_L) \tag{6}$$

the effective values become

$$C_{0L} = C_0(1 - \alpha) \tag{7}$$

$$k_L^2 = k^2(1 - \alpha). \tag{8}$$

Manuscript received October 16, 1977.
The author is with the U.S. Army Electronics Technology and Devices Laboratory (ERADCOM), Fort Monmouth, NJ 07703.

0018-9537/78/0700-0185$00.75

TABLE I
PHYSICAL AND ELECTRICAL PARAMETERS ASSOCIATED WITH AT-CUT QUARTZ RESONATORS

Quantity	Unit	Value
ρ	10^{+3} kg/m^3	2.649
ϵ	pF/m	39.82
$\bar{c}$	10^{+9} Pa	29.24
η	10^{-4} Pa · s	3.46
N	MHz - mm	1.661
$\lvert k \rvert$	%	8.80
τ_1	fs	11.8
r	---	159.4
Γ_1	fF/m	249.8
P_1	10^{-3} Ω-m	47.2
Ψ	---	0.6 - 0.9

Using k_L^2 in (5) yields the normalized load frequencies $X_{L0}^{(M)}$ and $f_{L0}^{(M)}$ in place of the corresponding resonance quantities. In the limit $\alpha \to 1$ ($C_L \to 0$), the load frequencies approach the antiresonance frequencies, while the limit $\alpha \to 0$ ($C_L \to \infty$) reduces the frequencies to the resonances.

The inclusion of loss is easily dealt with; if the loss is considered to arise from a material viscosity η, then substitution of

$$\hat{X} = X(1 - j\omega\eta/2\bar{c}) \tag{9}$$

for X in the foregoing describes the loss accurately. Table I gives a list of pertinent material constants for the AT-cut of quartz.

MASS-LOADING FREQUENCY EFFECTS

In normal practice the electrode coatings depress the frequency spectrum nonnegligibly. For coatings of mass m per unit area lumped on each surface, the reduced mass-loading variable is

$$\mu = m/\rho h. \tag{10}$$

With the inclusion of μ, (1) is replaced by

$$Y = j\omega C_0 \Big/ \left[1 - \left(\frac{k^2}{1 - \mu X \tan X} \right) \cdot \frac{\tan X}{X} \right]. \tag{11}$$

The zeros of (11) lead to the equation determining the antiresonances:

$$\mu X \tan X = 1. \tag{12}$$

The roots $X_{A\mu}^{(M)}$ of (12) are no longer harmonically related. From the $X_{A\mu}^{(M)}$ the frequencies of $f_{A\mu}^{(M)}$ are determined using (3).

The poles of (11) lead to the equation determining the resonance frequencies:

$$\tan X = X/(k^2 + \mu X^2). \tag{13}$$

The roots of (13) $X_{R\mu}^{(M)}$ determine the $f_{R\mu}^{(M)}$ from (3).

With C_L added in series to the mass-loaded vibrator, the quantities $X_{L\mu}^{(M)}$ and $f_{L\mu}^{(M)}$ are defined in an obvious way.

TABLE II
THERMAL PARAMETERS ASSOCIATED WITH AT-CUT QUARTZ RESONATORS

Quantity	Unit	Value
a_0	10^{-6}/K	0
b_0	10^{-9}/K^2	-0.45
c_0	10^{-12}/K^3	108.6
$\partial a/\partial\theta$	10^{-6}/K,$^o\theta$	-5.08
$\partial b/\partial\theta$	10^{-9}/K^2,$^o\theta$	-4.7
$\partial c/\partial\theta$	10^{-12}/K^3,$^o\theta$	-20.
$\partial^2 a/\partial\theta^2$	10^{-9}/K,$(^o\theta)^2$	0.96
$\partial a/\partial\phi$	10^{-6}/K,$^o\phi$	0
$\partial b/\partial\phi$	10^{-9}/K^2,$^o\phi$	0
$\partial c/\partial\phi$	10^{-12}/K^3,$^o\phi$	0
$\partial^2 a/\partial\phi^2$	10^{-9}/K,$(^o\phi)^2$	-18.0
$\partial a/\partial\mu$	10^{-6}/K,(%μ)	-0.24
T_1	^{o}C	26.4
$\partial T_1/\partial\theta$	K/$^o\theta$	14.9
$\partial T_1/\partial\mu$	K/(%μ)	-5.45
T_{Co}	10^{-6}/K	29.7
T_μ	10^{-6}/K	23.3
T_x	10^{-6}/K	-0.245
T_r	10^{-6}/K	-176.

Equation (12) is unaffected, while k^2 in (13) is replaced by k_L^2 from (8) to yield the load frequencies.

FREQUENCY-TEMPERATURE BEHAVIOR

Resonators for TCXO application are required to have precisely known frequency-temperature characteristics so that the compensatory network can be properly designed. Bechmann [10] found that AT-cut resonators could be described adequately, even over a wide temperature range, by a three-term power series. If the frequency of interest is f_0 at temperature T_0 (= 25°C), then with $\Delta T = T - T_0$,

$$(f - f_0)/f_0 = \Delta f/f_0 = a_0\Delta T + b_0\Delta T^2 + c_0\Delta T^3 \tag{14}$$

gives the frequency at temperature T. Table II gives values for the quantities a_0, b_0, and c_0 and their angle gradients for the AT-cut. The coefficients a_0, b_0, and c_0 vary with orientation angle, mass-loading, and value of series load capacitor with the zero subscripts denoting the values at zero μ and α, and at reference angles Φ_0, θ_0. The coefficient a is synonymous with T_{fR} appearing in the sequel.

Angular Dependence

The variation with angle is also treated by means of power series expansions, normally using only the constant and linear terms [11]:

$$q = q_0 + (\partial q/\partial\theta) \cdot \Delta\theta + (\partial q/\partial\Phi) \cdot \Delta\Phi \tag{15}$$

where q is a, b, or c, and $\Delta\theta = \theta - \theta_0$, $\Delta\Phi = \Phi - \Phi_0$. For the AT-cut, $\partial q/\partial\Phi \equiv 0$ due to crystal symmetry considerations, so the expansion in this case has to be carried out to second order [12]:

$$q = q_0 + (\partial q/\partial\theta) \cdot \Delta\theta + \tfrac{1}{2}(\partial^2 q/\partial\Phi^2) \cdot \Phi^2. \tag{16}$$

The normalized frequency excursion δf between the maximum and minimum of the curve of $\Delta f/f_0$ plotted against temperature is very important because δf enters directly into most TCXO design procedures. From the data in Table II and the relation

$$\delta f = 4(b^2 - 3ac)^{3/2}/27c^2 \tag{17}$$

the frequency excursion may be determined as a function of $\Delta\Phi$ and $\Delta\theta$. If δT is defined as the temperature interval corresponding to δf, then δT and δf are found to be related by the simple relation

$$\delta f = (c/2) \cdot (\delta T)^3 \tag{18}$$

where c is a weak function of orientation about the AT-cut angle. Equation (17) may be approximated for the AT-cut, in its explicit dependence upon $\Delta\theta$, by

$$\delta f \simeq 1.85 \times 10^{-6} \cdot (\Delta\theta)^{3/2}. \tag{19}$$

The corresponding relation for δT is

$$\delta T \simeq 32.5 \cdot (\Delta\theta)^{1/2} \tag{20}$$

where $\Delta\theta \geq 0$ is in minutes of arc.

Harmonic Effect

Changing the harmonic of operation is similar, as far as the resonance frequency-temperature behavior is concerned, to a change in apparent orientation angle, except that the harmonic effect is quantized.

The relation for the difference between the first-order temperature coefficients of the resonances and antiresonances was derived by Onoe [13], starting from (5); Bechmann [14] had earlier obtained an approximate relation. Equations for the higher-order differences were obtained recently [15]. For the first order we have

$$T_X = T_{fR0}^{(M)} - T_{fA0}^{(1)} = G_0^{(M)} \cdot T_k \tag{21}$$

where

$$G_0^{(M)} = +2k^2/((X_{R0}^{(M)})^2 + k^2(k^2 - 1)) \tag{22}$$

and where T_k is the first-order temperature coefficient of piezoelectric coupling. The harmonic effect arises from the root $X_{R0}^{(M)}$ appearing in (22). It is seen, from (21) and (22), that for $M >> 1$, $G_0^{(M)} \to 0$, and $T_{fR0} \to T_{fA0}$.

Load Capacitor Effect

Series load capacitor insertion is described in regard to its effect on k by (8); with respect to its influence on temperature behavior, (21) may be used with k_L^2 from (22), along with the relation between T_{kL} and T_k. This relation is found to be

$$2T_{kL} = 2T_k + \alpha(T_{CL} - T_{C0}) \tag{23}$$

so that the temperature behavior of C_L now comes into play, along with that of C_0. Values for T_{C0}, T_k, and T_X are given in Table II for the AT-cut. With α and k known, (22) can be used to find $G_0^{(M)}$ as a function of k_L.

The load capacitor effect on frequency-temperature behavior is shown in Fig. 1 for the AT-cut and a representative

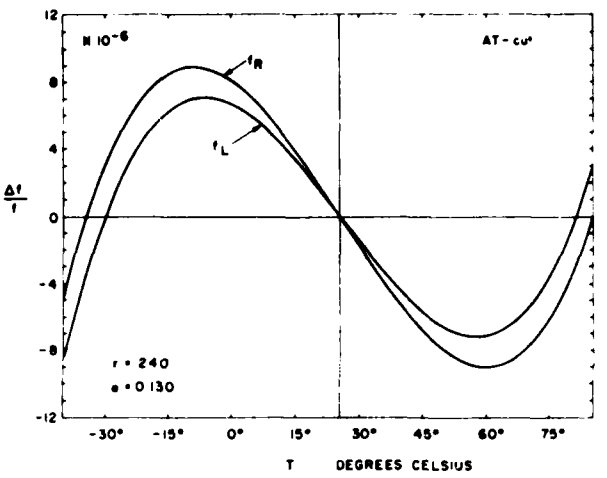

Fig. 1. Frequency-temperature characteristics of an AT-cut quartz vibrator with and without a series load capacitor. The presence of the capacitor reduces the peak-to-peak frequency deviation and makes the vibrator appear as if it had a reduced angle of cut.

value of α; we will return to this figure in connection with the numerical example presented later.

Mass-Loading Effect

Addition of mass-loading results in an expanded form of (21):

$$T_X = T_{fR\mu}^{(M)} - T_{fA\mu}^{(1)} = -(2k^2 \cdot T_k + \mu(X_{R\mu}^{(M)})^2 \cdot T_\mu)/D^{(M)} \tag{24}$$

where

$$D^{(M)} = (X_{R\mu}^{(M)})^4\mu^2 + (X_{R\mu}^{(M)})^2(2\mu k^2 + \mu + 1) + k^2(k^2 - 1). \tag{25}$$

T_μ is the temperature coefficient of the normalized mass-loading,

$$T_\mu = -T_\rho - T_h \tag{26}$$

T_ρ is the temperature coefficient of density and T_h is the temperature coefficient of expansion in the thickness direction.

The quantity multiplying T_k in (24) is the Onoe function:

$$G_\mu^{(M)} = +2k^2/D^{(M)}.$$

By means of (24) and the numerical value for $\partial\alpha/\partial\theta$ provided in Table II, one may convert changes in "α" due to changes in μ and/or M into apparent angle changes [16].

Inclusion of the C_L effect for the mass-loading case is made by writing (24) twice: once for $k = k_1$, $\mu = \mu_1$, and harmonic = N, and then for k_2, μ_2, and M, and subtracting. The result, with obvious abbreviations, is

$$\begin{aligned} T_{fR_{\mu 2}}^{(M)} - T_{fR_{\mu 1}}^{(N)} = {} & [-2k_2^2 T_{k2}/D_2^{(M)} + 2k_1^2 T_{k1}/D_1^{(N)}] \\ & + [-(\mu_2 X_{R\mu 2}^2/D_2)^{(M)} \\ & + (\mu_1 X_{R\mu 1}^2/D_1)^{(N)}] \cdot T_\mu. \end{aligned} \tag{28}$$

One now uses (8) and (23) to relate k_1 and k_2, T_{k1} and T_{k2}. Equation (28) then incorporates the full effects of changes of α, μ, and harmonic on the first-order resonance-frequency/temperature coefficient.

Equivalent Circuit Considerations

The equivalent circuit of Fig. 2 is usually used to represent a crystal resonator in the vicinity of a harmonic. C_0 is given by (2), while the remaining elements are [17]:

$$C_1^{(M)} = 8C_0k^2/\pi^2M^2 \tag{29}$$

$$R_1^{(M)} = \tau_1/C_1^{(M)} = \pi^2M^2\eta/8C_0k^2\bar{c} \tag{30}$$

and

$$L_1 = \pi M^2/32C_0k^2(f_{R0}^{(M)})^2. \tag{31}$$

The quantity τ_1 is the motional time constant [17], [18]. It is defined as

$$\tau_1 = \eta/\bar{c} \tag{32}$$

where η is the acoustic viscosity, and $\bar{c}$ is the piezoelectrically stiffened elastic constant. It is convenient to define two quantities that contain no geometrical factors, but which are functions of material only. These are the motional capacitance and motional resistance constants [19]:

$$\Gamma_1^{(M)} = C_1^{(M)} \cdot 2h/A = \epsilon/rM^2 \tag{33}$$

$$P_1^{(M)} = R_1^{(M)} \cdot A/2h = \tau_1/\Gamma_1^{(M)}. \tag{34}$$

In (33), r is the capacitance ratio

$$r^{(M)} = C_0/C_1^{(M)} = \tfrac{1}{2} \cdot (\pi M/2k)^2. \tag{35}$$

Table I lists values for $\epsilon, \bar{c}, \eta, \tau_1, r, \Gamma_1, P_1$, and $N = (\bar{c}/\rho)^{1/2}/2$; quantities appearing without a superscript (M) are for $M = 1$. The dimensionless number Ψ appearing in Table I is a form factor that takes into account the nonuniform distribution of motion with lateral distance along the plate [20]. The effective value of $C_1^{(M)}$ is just Ψ times the value obtained from (29); whereas $R_1^{(M)}$ is divided by Ψ to get the effective motional resistance. The static capacitance C_0 is not affected by the motional distribution.

Introduction of a series load capacitor alters C_0 according to (7); it also changes the other circuit parameters:

$$C_{1L}^{(M)} = C_1^{(M)}(1 - \alpha)^2 \tag{36}$$

$$R_{1L}^{(M)} = R_1^{(M)}/(1 - \alpha)^2 \tag{37}$$

$$L_{1L} = L_1/(1 - \alpha)^2 \tag{38}$$

$$r_L^{(M)} = r^{(M)}/(1 - \alpha). \tag{39}$$

From the definitions (29)–(35), the temperature coefficients of the circuit parameters may be obtained in terms of those of the material coefficients [21]. At present the quantity T_η is very imperfectly known.

While the lumped parameter circuit of Fig. 2 has been used to characterize the resonator, it is instructive to note that the exact network realization of (11) is that shown in Fig. 3 [22]. In this figure the crystal is represented by a bisected transmission line of electrical length κh and characteristic impedance $Z/2$, where

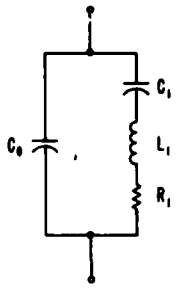

Fig. 2. Butterworth–Van Dyke equivalent circuit of a vibrating crystal. The circuit is an adequate representation in the vicinity of any single resonance.

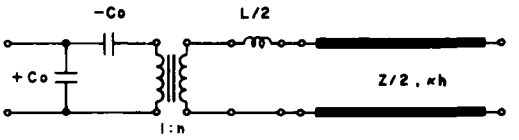

Fig. 3. Broad-band transmission line equivalent circuit of a vibrating crystal. This circuit holds for all resonances belonging to the single mode characterized. The lumped inductor represents the effect of mass loading.

$$\kappa h = X, (\hat{X} \text{ in the lossy case}) \tag{40}$$

and

$$Z/2 = A\rho N. \tag{41}$$

Electrode mass-loading produces an inductor of value

$$L/2 = A\rho\mu h/2. \tag{42}$$

The piezoelectric transformer turns ratio n is given by

$$n = (2C_0Zk^2f_{A0}^{(1)})^{1/2}. \tag{43}$$

Fig. 2 is recovered from Fig. 3 by a partial-fractions expansion of the tangent function represented by the transmission line, the realization of the expansion terms as lumped shunt branches, and the retention of the single branch appropriate to the harmonic of interest. The presence of the $-C_0$ element in Fig. 3 renders (36) and (39) exact, whereas by starting from Fig. 2 they would be approximate.

Frequency-Temperature-Load Capacitance Approximations

Dependence of $G_\mu^{(M)}$ on μ is very weak until μ exceeds several percent; accordingly, it is usually acceptable to let $G_\mu^{(M)} = G_0^{(M)}$. The zeroth approximation to $G_0^{(M)}$ is

$$G_0^{(M)} \simeq +2k^2/(\pi M/2)^2 = 1/r^{(M)} \tag{44}$$

the first approximation is

$$G_0^{(M)} \simeq +2k^2/[(\pi M/2)^2 - k^2]. \tag{45}$$

The presence of μ only enters the second approximation:

$$G_\mu^{(M)} \simeq +2k^2 \Big/ \left\{(\pi M/2)^2\left[1 - \mu - \left(\frac{2k}{\pi M}\right)^2\right]^2 + k^2(k^2 - 1)\right\}. \tag{46}$$

By making approximations of the sort found in (44)-(46), (28) may be reduced to various simpler forms. When $\alpha = 0$ and $\mu = 0$, one has

$$T_{fR0}^{(M)} - T_{fR0}^{(N)} = (T_r/2r) \cdot (1/M^2 - 1/N^2) \tag{47}$$

where

$$T_r = -2T_k. \tag{48}$$

If $\mu_1 \neq \mu_2, M \neq N$, then with the addition of C_L the exact result is

$$\begin{aligned} T_{fR\mu 2}^{(M)} - T_{fL\mu 1}^{(N)} = -2k^2 T_k \; & [(1-\alpha)/D_2^{(M)} - 1/D_1^{(N)}] \\ & -k^2\alpha(1-\alpha)(T_{CL} - T_{C0})/D_2^{(M)} \\ & - [(\mu X_R^2/D)_2^{(M)} - (\mu X_R^2/D)_1^{(N)}] \cdot T_\mu. \end{aligned} \tag{49}$$

The most important practical case is that where $\mu_2 = \mu_1 = \mu$, $N = M$. Then, for the shift in first-order temperature coefficient between resonance and load frequencies we have, approximately,

$$\begin{aligned} (T_{fR\mu} - T_{fL\mu}) \simeq + \frac{\alpha}{2rM^2} \{ & (1+2\mu)[T_r + (1-\alpha) \\ & \cdot (T_{CL} - T_{C0})] + 2\mu \cdot T_\mu \}. \end{aligned} \tag{50}$$

For small μ this further reduces to

$$(T_{fR0} - T_{fL0}) \simeq \frac{+\alpha}{2rM^2} \cdot [T_r + (1-\alpha) \cdot (T_{CL} - T_{C0})]. \tag{51}$$

Use of At-Cut Quartz Resonators for TCXO Applications

By use of (13), (8), and the definition (3), simple approximate relations may be found for the frequency shift between the load and resonance frequencies. Provided $M\mu \ll 1$, the result is very insensitive to μ. We omit unnecessary subscripts in the following. The frequency shift is

$$(f_L^{(M)} - f_R^{(M)})/f_R^{(M)} = \Delta f/f \simeq (2k/\pi M)^2 \cdot \alpha = \alpha/(2rM^2). \tag{52}$$

For TCXO application, the fundamental ($M = 1$) is used to provide the greatest range for Δf (maximum "pullability"). Since the quantity $1/(2r)$ greatly exceeds δf for TCXO's, it is apparent that only small variation in C_L about its operating point is ordinarily sufficient to bring about the necessary frequency compensation.

Two important questions now arise: one concerns the shift in frequency-temperature behavior of the resonator in going from the condition of f_R to f_L; the other concerns the smaller shifts in the frequency-temperature characteristic attendant on the variations of C_L about its initial setting point. The further effects of μ are also open to question. These points will now be taken up and considered from the standpoint of a practical example.

Consider an AT-cut crystal resonator with the following characteristics:

- $f_R = 20$ MHz, $M = 1$
- $C_0 = 3.0$ pF
- $C_1 = 12.5$ fF
- $R_1 = 4\Omega$
- $\mu = 2$ percent
- $\Delta\theta \simeq 4\frac{1}{2}$ minutes of arc.

From Table II, this $\Delta\theta$ value corresponds approximately to

$$\delta f_R \simeq 18 \times 10^{-6}, \quad \delta T \simeq 69.4^\circ\text{C}$$

stemming from the temperature coefficients

$$a = -0.386 \times 10^{-6}/\text{K}$$
$$b = +0.038 \times 10^{-9}/\text{K}^2$$
$$c = +108.0 \times 10^{-12}/\text{K}^3.$$

Fig. 1 presents the behavior of the resonance frequency f_R with temperature. Operation with series load capacitor

- $C_L = 20$ pF

at the frequency at which the combination exhibits zero reactance produces, as function of temperature, the curve marked f_L in Fig. 1, assuming $(T_{CL} - T_{C0})$ vanishes. The f_L curve is characterized by

$$\alpha = C_0/(C_0 + C_L) = 0.130$$

and capacitance ratio

$$r = C_0/C_1 = 240.$$

Ratios α and r are inserted into (51) to yield the new first-order coefficient.

$$a = -0.332 \times 10^{-6}/\text{K}.$$

Coefficients b and c remain unchanged to good approximation, but with the a coefficient change the curve is made to appear with shifted angle difference

$$\Delta\theta \simeq 4 \text{ minutes of arc}$$

and hence

$$\delta f_L \simeq 15 \times 10^{-6}, \quad \delta T \simeq 65.4^\circ\text{C}.$$

According to (37) the resistance of the combination is now

$$R_{1L} = R_1/(1-\alpha)^2 \simeq 5.3\ \Omega.$$

Schodowski [23] has found the coefficient a to shift by an amount comparable to that calculated above. A definitive comparison is not possible in this case because several experimental data, particularly T_{CL}, are unavailable.

If (17) is used, with a taken to depend upon α according to (50), then δf_L may be plotted against α for assumed values of $(T_{CL} - T_{C0})$ and μ. The resulting graphs are shown in Fig. 4 for values pertinent to the example described above. In addition to the C_L value quoted (20 pF), two further values are indicated on the figure:

- $C_L = 22$ pF, $\alpha = 0.120$

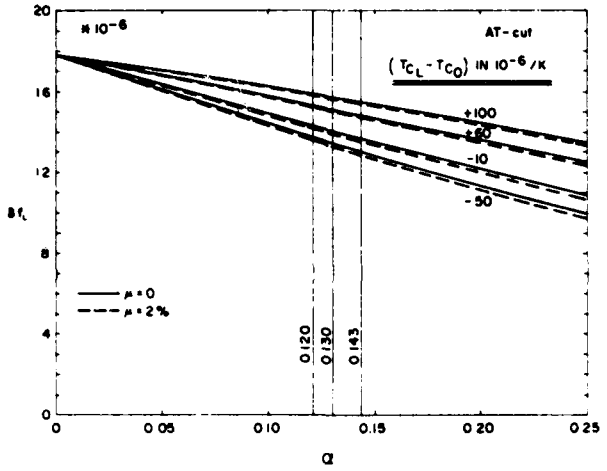

Fig. 4. Peak-to-peak frequency deviation plotted against load capacitance parameter α. The values shown are pertinent to the example given in the text.

and

- $C_L = 18$ pF, $\alpha = 0.143$.

Graphs are plotted in Fig. 4 for the following values of $(T_{CL} - T_{C0})$: -50, -10, +60, and +100 (all $\times 10^{-6}$/K), with and without the presence of 2 percent mass-loading. Inasmuch as the nominal value of T_{C0} for AT-cut quartz is

$$T_{C0} \simeq +30 \times 10^{-6}/\mathrm{K}$$

(see Table II), the assumed values of T_{CL} are ±20, + 90, and + 130 (all $\times 10^{-6}$/K).

These numbers correspond, respectively, to the nominal temperature coefficient values for ceramic capacitors, for porcelain microcircuit capacitors, and for certain oscillator-varactor composites. Table III provides the δf_L values for the intersections of the three α values with the four $(T_{CL} - T_{C0})$ graphs, in the absence of μ. From Fig. 4 and Table III, the relative sizes of the influences on δf_L may be discerned.

Using the exact relation (49), the plots of Fig. 4 are extended in Figs. 5 and 6 to encompass the full range of α. These are for AT-cut crystals operating on the fundamental harmonic with capacitance ratio

$$r = 240$$

angle shifts

$$\Delta\theta = 1\ (10)\ 10 \text{ minutes of arc}$$

and capacitance temperature coefficient differences

$$(T_{CL} - T_{C0}) = -100\ (50)\ 100 \times 10^{-6}/\mathrm{K}.$$

Because the graphs for each value of $\Delta\theta$ conflue at $\alpha = 0$ and $\alpha = 1$, irrespective of $(T_{CL} - T_{C0})$, the resulting design charts are denoted as "petal plots." By the use of this type of chart, the shift of δf with α may be determined and taken into account in TCXO applications. Additional considerations may be found in [24].

TABLE III
PEAK-TO-PEAK FREQUENCY DEVIATIONS $\delta f_L(10^{-6})$

$T_{CL}-T_{Co}$ $(10^{-6}/K)$	$\alpha = C_0/(C_0 + C_L)$		
	0.120	0.130	0.143
-50	12.3	11.9	11.4
-10	13.1	12.7	12.3
+60	14.6	14.3	14.0
+100	15.5	15.3	15.0

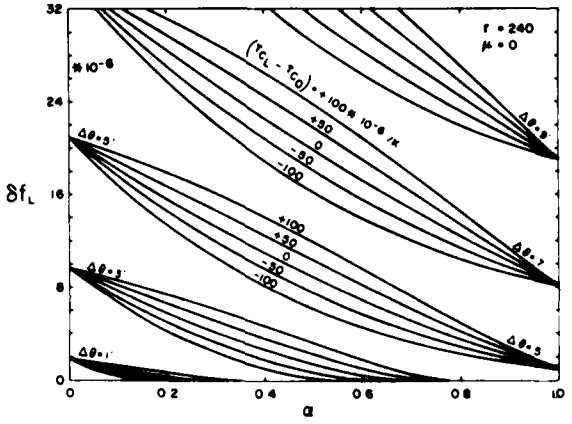

Fig. 5. Petal plots of peak-to-peak frequency deviation plotted against load capacitance parameter α for odd values of crystal angle $\Delta\theta$.

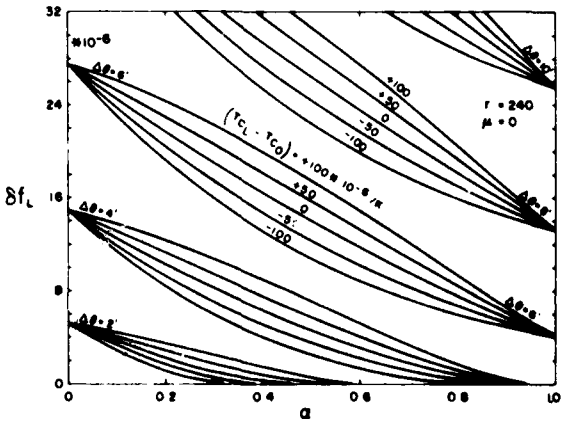

Fig. 6. Petal plots of peak-to-peak frequency deviation plotted against load capacitance parameter α for even values of crystal angle $\Delta\theta$.

Conclusions

Resonators for TCXO application are required to have accurately characterized frequency-temperature (f - T) curves and equivalent network parameters. This paper describes how the circuit parameters, critical resonator frequencies, and temperature coefficients depend on material constants of the crystal and geometrical factors. It further explains the observed f - T curve shift between resonator operation with and without series load capacitors. Simple relations are given for treating this effect. A practical example involving an AT-cut resonator for a typical TCXO application is also given.

References

Note: Many of the references were presented at the Annual Frequency Control Symposium, US Army Electronics R & D Command, Fort Monmouth, NJ 07703. They are cited here as AFCS for brevity.

[1] G. R. Hykes and D. E. Newell, "A temperature-compensated frequency standard," Proc. 15th AFCS, May 1961, pp. 297-317.

[2] D. E. Newell, H. Hinnah, and R. Bangert, "Advances in crystal oscillator and resonator compensation," Proc. 18th AFCS, May 1964, pp. 487-534.

[3] D. E. Newell and H. Hinnah, "A report on TCXO's and segmented compensation," Proc. 23rd AFCS, May 1969, pp. 187-191.

[4] S. Schodowski, "A new approach to a high stability temperature compensated crystal oscillator," Proc. 24th AFCS, April 1970, pp. 200-208.

[5] P. C. Duckett, R. J. Peduto, and G. V. Chizak, "Temperature compensated crystal oscillators," Proc. 24th AFCS, April 1970, pp. 191-199.

[6] G. E. Buroker and M. E. Frerking, "A digitally compensated TCXO," Proc. 27th AFCS, June 1973, pp. 191-198.

[7] D. L. Thomann, "A microcircuit temperature compensated crystal oscillator (MCTCXO)," Proc. 28th AFCS, May 1974, pp. 214-220.

[8] A. B. Mroch and G. R. Hykes, "A miniature high stability TCXO using digital compensation," Proc. 30th AFCS, June 1976, pp. 292-300.

[9] M. Onoe, H. F. Tiersten, and A. H. Meitzler, "Shift in the location of resonant frequencies caused by large electromechanical coupling in thickness-mode resonators," J. Acoust. Soc. Am., Vol. 35, January 1963, pp. 36-42.

[10] R. Bechmann, "Frequency-temperature-angle characteristics of AT-type resonators made of natural and synthetic quartz," Proc. IRE, Vol. 44, November 1956, pp. 1600-1607.

[11] R. Bechmann, "Frequency-temperature-angle characteristics of AT- and BT-type quartz oscillators in an extended temperature range," Proc. IRE, Vol. 48, August 1960, p. 1494.

[12] A. Ballato and G. J. Iafrate, "The angular dependence of piezoelectric plate frequencies and their temperature coefficients," Proc. 30th AFCS, June 1976, pp. 141-156.

[13] M. Onoe, "Relationship between temperature behavior of resonant and antiresonant frequencies and electromechanical coupling factors of piezoelectric resonators," Proc. IEEE, Vol. 57, April 1969, pp. 702-703.

[14] R. Bechmann, "Influence of the order of overtone on the temperature coefficient of frequency of AT-type quartz resonators," Proc. IRE, Vol. 43, Nov. 1955, pp. 1667-1668.

[15] A. Ballato and T. Lukaszek, "Higher-order temperature coefficients of frequency of mass-loaded piezoelectric crystal plates," Proc. 29th AFCS, May 1975, pp. 10-25.

[16] A. Ballato, "Apparent orientation shifts of mass-loaded plate vibrators," Proc. IEEE, Vol. 64, September 1976, pp. 1449-1450.

[17] A. Ballato, "Doubly rotated thickness mode plate vibrators," in *Physical Acoustics* (W. P. Mason and R. N. Thurston, eds.), Vol. 13, 1977, Academic Press, pp. 115-181.

[18] G. K. Guttwein, T. J. Lukaszek, and A. Ballato, "Practical consequences of modal parameter control in crystal resonators," Proc. 21st AFCS, April 1967, pp. 115-137.

[19] R. Bechmann, "Schwingkristalle für Siebschaltungen," Archiv d. elektr. Übertragung, Vol. 18, February 1964, pp. 129-136.

[20] R. Bechmann, "Über Dickenschwingungen piezoelektrischer Kristallplatten," Archiv d. elektr. Übertragung, Vol. 6, September 1952, pp. 361-368.

[21] E. Hafner, "Crystal resonators," IEEE Trans. Sonics Ultrason., Vol. SU-21, October 1974, pp. 220-237.

[22] A. Ballato, H. L. Bertoni, and T. Tamir, "Systematic design of stacked-crystal filters by microwave network methods," IEEE Trans. Microwave Theory Tech., Vol. MTT-22, January 1974, pp. 14-25.

[23] S. Schodowski, "Design of a high stability voltage controlled crystal oscillator," Technical Report ECOM-3532, US Army Electronics Command, Fort Monmouth, NJ, February 1972, 29 pp.

[24] A. Ballato, "Temperature compensated crystal oscillator (TCXO) design aids: frequency-temperature resonator characteristics as shifted by series capacitors," Technical Report ECOM-4498, US Army Electronics Command, Fort Monmouth, NJ, May 1977, 59 pp.